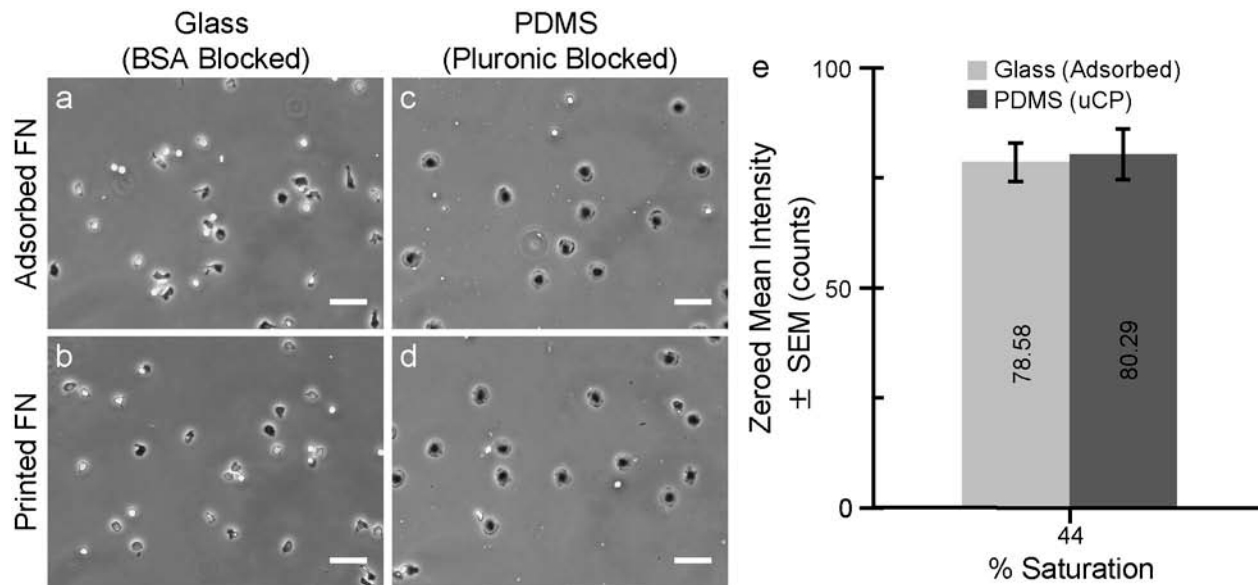


## Supplementary Materials

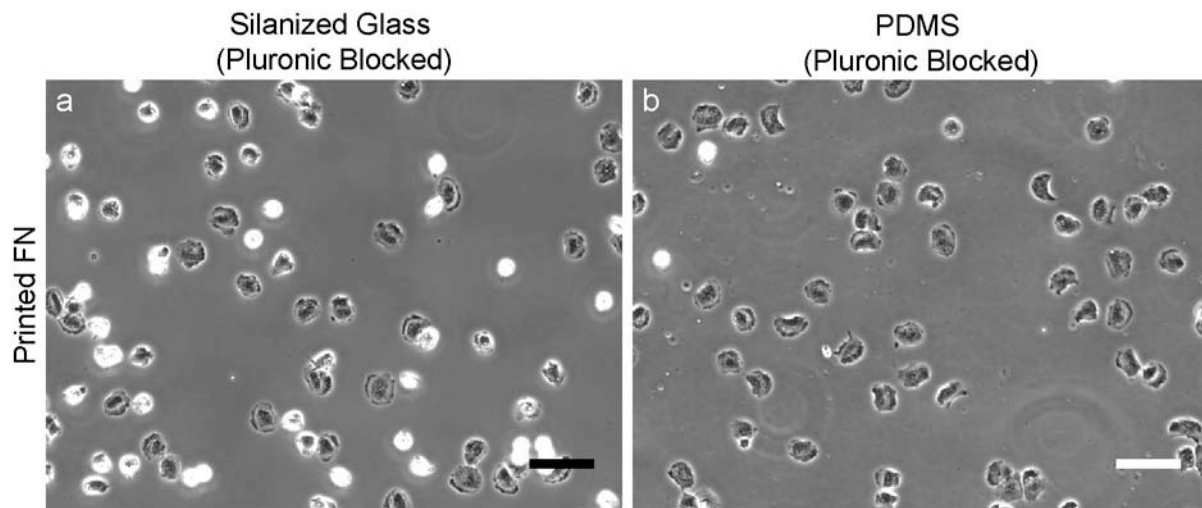
### Ligand density elicits phenotypic switch in human neutrophils

Steven J. Henry, John C. Crocker, and Daniel A. Hammer



**Supplementary Fig. 1 Phenotype does not follow method of protein deposition.** To determine if method of protein deposition dictated the two cell phenotypes we compared the following surface preparation strategies: (a) FN-adsorbed glass, BSA blocked (reproduced from Fig. 1a of main text), (b) FN-printed glass, BSA blocked, (c) FN-adsorbed PDMS, Pluronic blocked, and (d) FN-printed PDMS, Pluronic blocked (reproduced from Fig. 1b of main text). Scalebars = 50  $\mu\text{m}$ . Phenotype followed the method of blocking not the method of FN deposition. (e) Mean intensity of FN594 (FN conjugated to Alexa Fluor 594 dye) adsorbed onto glass and printed onto PDMS. Images were acquired under identical settings and the mean pixel intensity computed. For each preparation, the mean pixel intensity of the corresponding negative control was subtracted to produce the “zeroed mean intensity”. Error bars are  $\pm$  standard error of the mean ( $n = 2$  independent experiments). Amount of deposited FN on both surfaces is comparable.

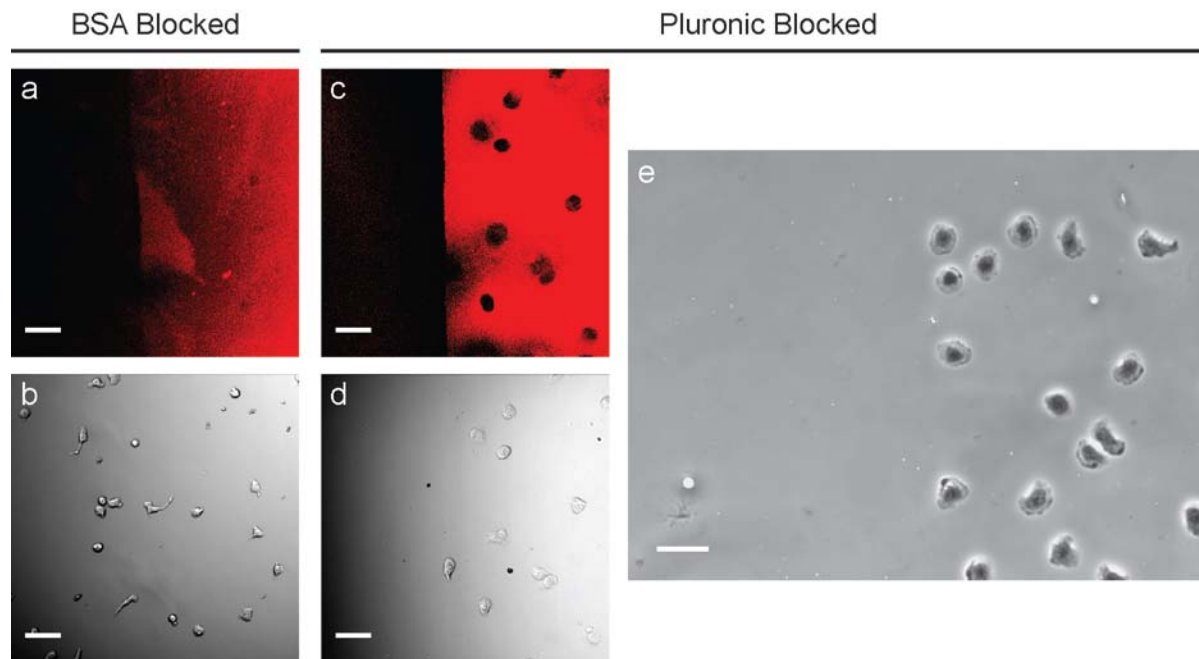
## Supplementary Materials



**Supplementary Fig. 2 Keratocyte-like phenotype recapitulated on Pluronic-blocked glass.**

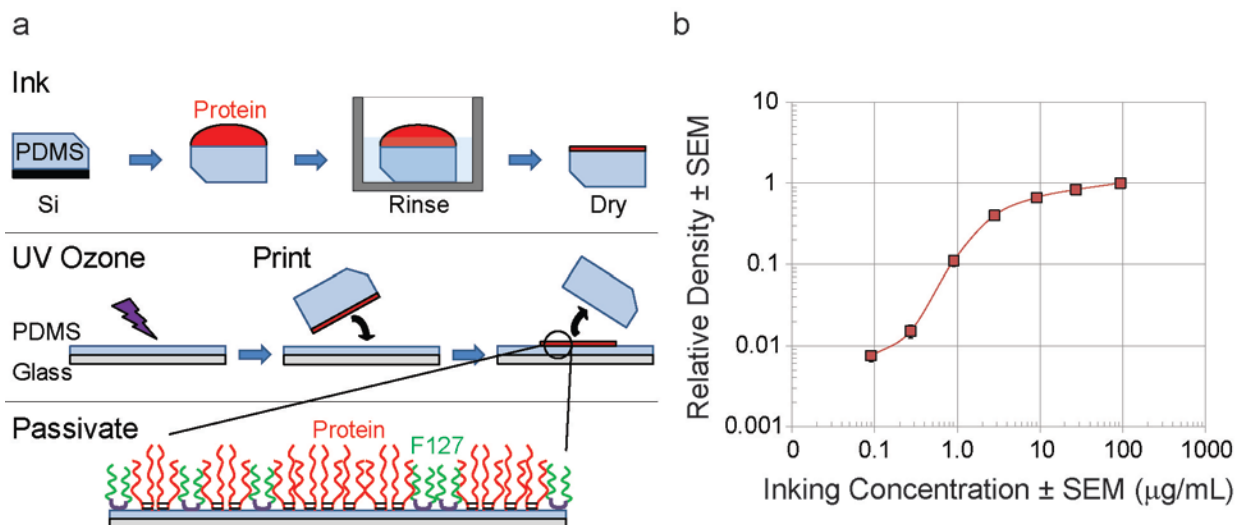
To determine if substrate type (i.e. glass vs. PDMS) dictated the two cell phenotypes we performed the following controls: (a) FN-printed silanized glass, Pluronic blocked (b) FN-printed PDMS, Pluronic blocked. Surfaces functionalized at 40% FN-surface saturation. Scalebars = 50  $\mu\text{m}$ .

## Supplementary Materials



**Supplementary Fig. 3 Exquisite cell-ligand specificity on Pluronic blocked substrates.** Pluronic F-127 blocking of PDMS substrates allows complete inhibition of non-specific binding in human neutrophils. (a) FN conjugated to Alexa Fluor 647 (FN647) after adsorption to a piranha cleaned coverslip, blocked with 0.2% BSA in PBS (w/v). The distinct edge shown was achieved by affixing a single-well flexiPERM gasket to the coverslip which was removed prior to blocking and cell plating. (b) DIC image of fixed human neutrophils in same location as (a). Observe that cell adhesion is seen in regions of the substrate not functionalized with FN. (c) FN647 after printing on a PDMS spin-coated coverslip, blocked with 0.2% Pluronic F-127 in PBS (w/v). (d) DIC image of fixed human neutrophils on microcontact printed substrate in same location as (c). No adhesion outside of the functionalized area is observed. (e) Phase contrast image of fixed cells at a different edge location on same substrate (c-d). All scale bars are 40  $\mu\text{m}$ . Note: non-uniform image acquisition parameters preclude comparison of fluorescent signal intensities between the glass and PDMS conditions (a, c). Surfaces functionalized at 40% FN surface saturation.

## Supplementary Materials



**Supplementary Fig. 4 Microcontact printing overview and sub-saturating density quantification.** (a) PDMS is cast against a silicon wafer to generate a smooth inking face. Stamps are trimmed and a sessile drop of protein solution at known concentration is used to coat the smooth stamping face. Stamps are rinsed and dried gently in a stream of nitrogen. Separately PDMS-spun coverslips are rendered hydrophilic by exposure to UV ozone for 7 min. When the inked stamps are brought into contact with the spun coverslip there is preferential transfer of the protein from the natively hydrophobic stamp to the hydrophilic coverslip. Finally the substrate is passivated by submersion in a nonionic triblock copolymer sold under the tradename Pluronic F127. Bare regions of the PDMS not occupied by adhesive ligand are rendered stealth to neutrophils by Pluronic coating. (b) Quantitative fluorescence microscopy to determine the relative density of protein on printed substrates by titrating inking concentration. The saturating condition was considered to be 100 µg/mL. Error bars are standard error of the mean ( $n = 7-9$  independent experiments).

# Supplementary Materials

## Flow Cytometry to Assess Activation State

Because neutrophils were robustly haptokinetic on FN alone without the addition of chemoattractant, we verified that cells were not primed for binding to the adhesion ligand as a result of stresses experienced prior to FN exposure. We used L-selectin as the marker of cell activation state. Kishimoto and coworkers demonstrated that L-selectin is a sensitive marker of a neutrophil's transition from quiescence to a phenotype primed for integrin-mediated binding<sup>1</sup>, a transition denoted by rapid L-selectin shedding.

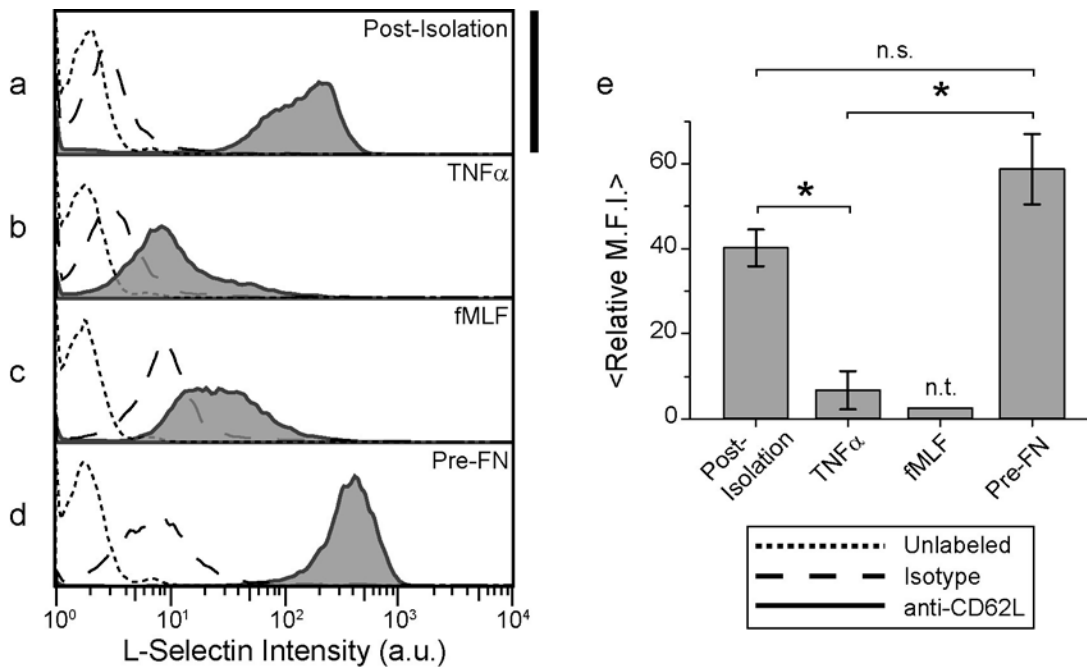
Staining of all treatment conditions was for 45 min on ice in the dark immediately followed by fixation in 2% formaldehyde for 20 min. After fixation, vials were spun to pellet cells (350 xg, 5 min, 4°C) and resuspended in HBSS without calcium or magnesium. This rinsing sequence was repeated three times. After the final resuspension, cells were stored overnight on ice in the dark until flow cytometry measurements the following day. Antibodies were mouse-anti-human CD62L-PE-Cy5 (eBioscience) and mouse IgG1κ-PE-Cy5 isotype control (eBioscience).

Immediately after isolation, neutrophils were stained for L-selectin (Supplementary Fig. 5a). Positive (i.e. activated) controls were generated by exposing isolated neutrophils to the chemoattractants TNF $\alpha$  and fMLF immediately following isolation (Supplementary Fig. 5b,c). A decrease in L-selectin expression by cells exposed to chemoattractant, relative to the post-isolation control, demonstrated the isolated neutrophils had the capacity to be activated. To mimic the conditions cells would experience prior to plating on a FN-printed PDMS substrate, a separate aliquot of cells was subjected to storage, buffer exchange, and re-warming consistent with the plating protocol used in our motility studies. Flow cytometry on these pre-FN mimics

## Supplementary Materials

(Supplementary Fig. 5d) showed a slight increase in L-selectin expression relative to the post-isolation control.

To quantify the extent of these shifts, the relative median fluorescence intensity (Relative M.F.I. =  $(M.F.I._{Isotype} - M.F.I._{Sample})/M.F.I._{Isotype}$ ) of each condition was computed (Supplementary Fig. 5e). A statistically significant decrease in L-selectin expression as a function of  $TNF\alpha$  was observed relative to the post-isolation control and pre-FN mimic. No statistically significant difference was found between the post-isolation control and pre-FN condition. Thus while the isolated neutrophils were capable of activation, they were not primed for integrin-mediated binding by virtue of isolation or storage stresses prior to FN exposure. This finding, coupled with high cell-FN specificity on Pluronic blocked PDMS substrates, leads us to attribute the post-plating adhesion and haptokinesis solely to the deposited FN.

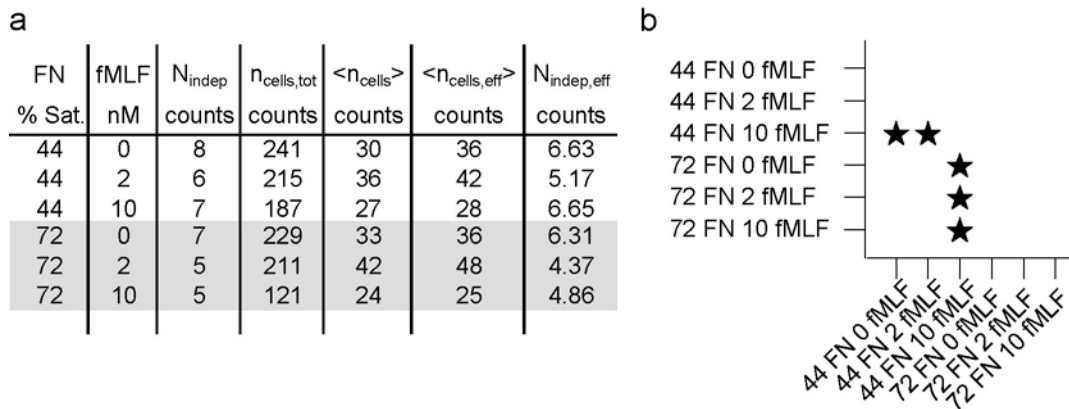


**Supplementary Fig. 5 Quantification of L-selectin expression levels via flow cytometry.** Expression levels were assayed under the following conditions: (a) immediately after isolation from whole blood, (b) immediately after isolation including 100 U/mL  $TNF\alpha$  or (c) 100 nM fMLF as positive activation controls, and (d) prior to FN exposure mimicking the storage, buffer exchange, and re-warming steps experienced by plated cells. Scalebar is 400 counts. Mean relative median fluorescence intensity (Relative M.F.I) was computed for each experimental

## Supplementary Materials

condition (e). Errorbars are standard error of the mean ( $n = 2$  donors). Asterisk denotes significant difference and n.s. denotes a difference not statistically significant as computed by post-hoc SNK Multiple Comparisons Method ( $p < 0.05$ ). fMLF was excluded from significance testing (n.t.).

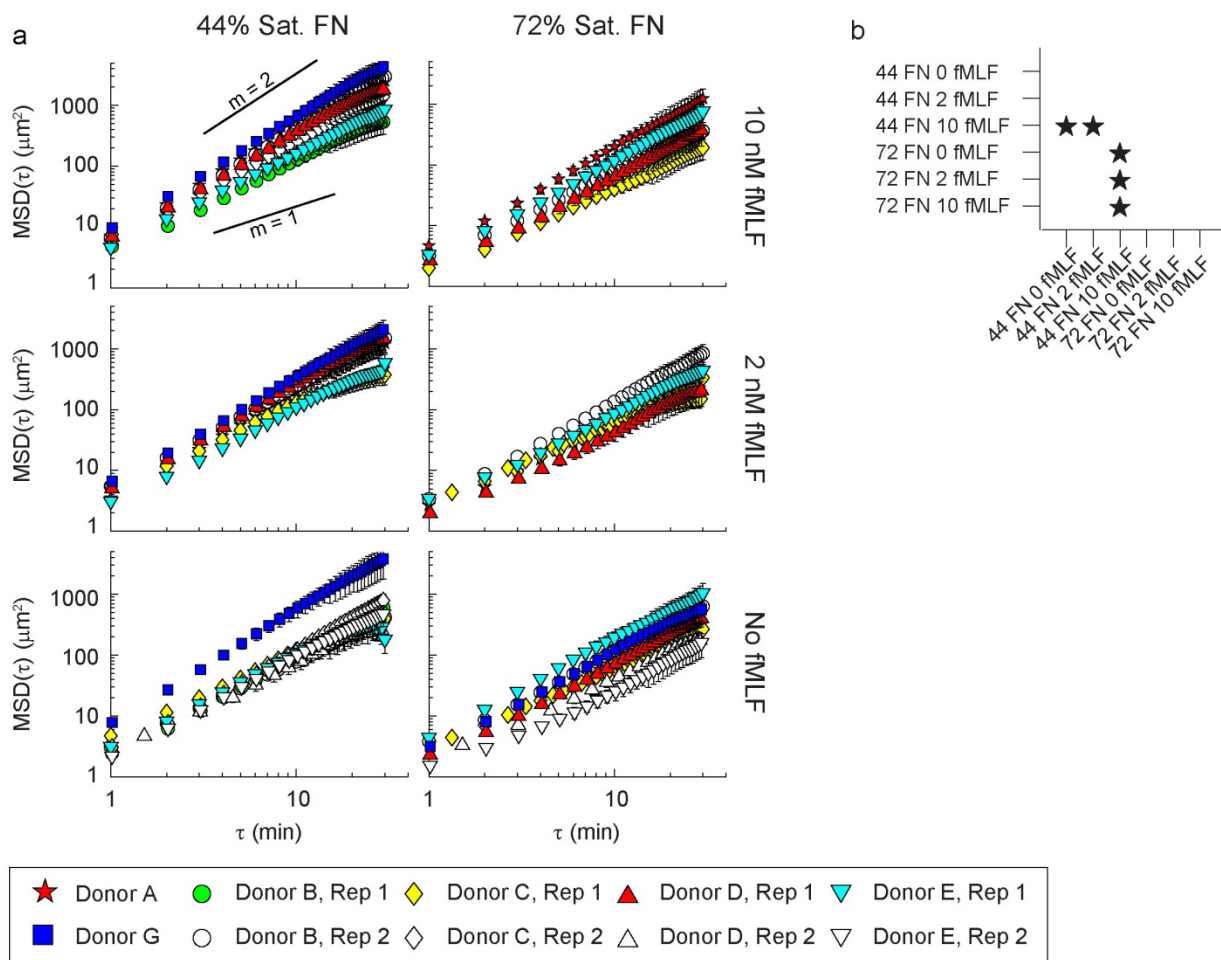
# Supplementary Materials



**Supplementary Fig. 6 Table of sample sizes per condition and complete results of model-independent significance testing.** (a) Table summarizing sample sizes for each experimental condition (FN/fMLF combination).  $N_{\text{indep}}$  (column 3) is the number of independent observations where an independent observation is a unique donor/donation combination.  $N_{\text{cells,tot}}$  (column 4) is the number of total cell trajectories acquired across all independent observations.  $\langle n_{\text{cells}} \rangle$  (column 5) is the average number of cells contributed by each independent observation without weighting. Because each independent observation of a condition contributed a different number of cells, weighting is required. Weighting mean values by the number of cells used in the computation of the mean results in an effective number of independent observations on the mean given by  $N_{\text{indep,eff}}$  (column 7) and a corresponding effective average number of cells per independent observation  $\langle n_{\text{cells,eff}} \rangle$  (column 6). These later two values can be thought of as a hypothetical number of independent observations ( $N_{\text{indep,eff}}$ ) of equal statistical power, each experiment contributing the same number of cells ( $\langle n_{\text{cells,eff}} \rangle$ ). (b) Complete results of significance testing corresponding to the mean maximum displacement metric of Fig. 4c in the main text. A star denotes a significance difference as computed by post-hoc SNK Multiple Comparisons Method ( $p < 0.05$ ).



## Supplementary Materials



**Supplementary Fig. 7 MSDs of all independent observations of FN/fMLF experimental conditions tested.** (a) For a given elapsed time interval ( $\tau$ ),  $\text{MSD}(\tau)$  is the variance of the population of displacements within and across all cells (i.e. time and ensemble averaged).  $\tau_{\min}$  is the experimental frame rate and  $\tau_{\max}$  is 30 min. This study utilized six donors (closed symbols), four of which donated on a separate experimental day (open symbols). Variability within a given donor on different experimental days for the same experimental condition led us to treat each donor/donation as an independent observation. Plots are organized by adhesiveness (columns) and concentration of fMLF (rows). All plots are scaled identically. Error bars are  $\pm$  standard error of the variance (i.e. of the  $\text{MSD}(\tau)$ ). Eye guides of slope (“ $m$ ”) 1 and 2 are provided for reference. (b) Complete results of significance testing corresponding to the speed parameter “ $S$ ” from the persistent random walk fit to the empirical MSDs. A star denotes a significance difference as computed by post-hoc SNK Multiple Comparisons Method ( $p < 0.05$ ). No statistically significant differences were found among persistence values of Fig. 4e.

# Supplementary Materials

**Supplementary Movie S1 Amoeboid phenotype.** Human neutrophil haptokinesis on 44% surface-saturated FN, adsorbed to glass, blocked with BSA.

**Supplementary Movie S2 Keratocyte-like phenotype.** Human neutrophil haptokinesis on 44% surface-saturated FN, printed PDMS, blocked with Pluronic F-127. Neutrophils are from same donation as Movie 1.

## References:

1. T. K. Kishimoto, M. A. Jutila, E. L. Berg, E. C. Butcher, Neutrophil Mac-1 and MEL-14 adhesion proteins inversely regulated by chemotactic factors. *Science* 1989, 245. 1238-41, DOI: 10.1126/science.2551036.